Marine and Petroleum Geology 98 (2018) 397–400

Contents lists available at ScienceDirect

Marine and Petroleum Geology

journal homepage: www.elsevier.com/locate/marpetgeo

Shear heat model for gouge free dip-slip listric normal faults

Soumyajit Mukherjee[a,*], Ishiqua Agarwal[b]

[a] Department of Earth Sciences, Indian Institute of Technology Bombay, Powai, Mumbai, 400 076, Maharashtra, India
[b] Department of Geological Sciences, Indian Institute of Technology Kharagpur, Kharagpur, 721 302, West Bengal, India

ARTICLE INFO

Keywords:
Shear heat
Frictional heat
Listric fault
Brittle shear
Structural geology

ABSTRACT

Shear heating due to brittle faulting is important in petroleum geosciences, tectonics and seismic studies. Temporal variation of shear heat in a listric normal fault, with a circular arc-shaped fault plane is simulated in this work, which was not done so far. The work is expected to have a far reaching implication in tectonics and petroleum geosciences since listric faults can be closely associated with hydrocarbon reserves (e.g., Valdiya and Sanwal, 2017). For such a fault plane devoid of gouge and any secondary faulting, shear heat is proportional to the mass of the hanging-wall block, the coefficient of friction acting between the hanging-wall and the footwall block, and radius of the circular arc. Shear heating intensifies temporally as the hanging wall block slides down and reaches progressively gentler fault dip.

1. Introduction

"The detection of frictional heating effects along faults provides key insight into the dynamics of earthquakes and faulting"- M. Kitamura et al. (2012).

Modeling and estimation of shear/frictional heating along brittle planar fault planes/zones have been studied in tectonics (e.g., Hamada et al., 2009; Mukherjee, 2017; Mukherjee and Khonsari, 2017, 2018). Seismicity can reactivate a fault for few seconds. This can produce shear heating significant enough to get recorded in terms of young apatite age deduced from the fault gauge (Yamada et al., 2009). In several cases, fault-related shear heating have been linked with thermal maturation of hydrocarbon (Underwood et al., 1988a; b; Sakaguchi et al., 2007). Also, coal can mature within tens of seconds due to fault's frictional heating ranging 26–266 °C (Kitamura et al., 2012). Shear heating can be deciphered physically from thermal aureoles/partial melting/pseudotachylite found at fault planes, or chemically by studying biomarkers present in the sedimentary rock close to the fault (Savage et al., 2014).

However, we do not understand the shear heating mechanism and the resulting heat anomaly for all kinds of faults and in several tectonic regimes yet. For example, how far thermal anomaly can be produced in rift setting has been questioned (Bertotti and ter Voorde, 1994). To estimate thermal budget for normal faulting, its shear heat component needs to be computed (Grasemann and Mancktelow, 1993). Thermal anomalies associated to faulting have been investigated in petroleum geosciences, sometimes without considering at all the effect of brittle shear heating (such as Wüstefeld et al., 2017), which therefore does not appear to be a correct approach. In particular, frictional heat estimation has not yet been done for curved/listric faults, common in rift basins and passive margins (Shelton, 1984).

Listric faults (e.g., Fig. 3.19 of Mukherjee, 2013a, 2014a, 2015, Fig. 14 of Dasgupta and Mukherjee, 2017) are generally concave in geometry, with downward decreasing dip magnitude. At some depth such faults merge with sub-surface regional detachment faults. Such a listric geometry of faults are also common in collisional mountains, such as the Himalaya (Mukherjee, 2013b; Mandal et al., 2015) and the Zagros. Rarely listric faults can have convex-up geometries, and are the called anti-listric/cylindrical faults (Hills, 2012). Listric fault activity can significantly raise temperature due to frictional/shear heating leading to pseudotachylite formation (Theunissen et al., 2002). Modeling estimates of shear heating due to listric faulting would be important in petroleum geosciences (Harding and Lowell, 1979) since such faults (and their associated reverse drag folds: Mukherjee, 2014b) can act specifically as pathways (and as traps) for hydrocarbons. Several modes of listric faulting have been available (Fossen, 2016). This work does not investigate the mode of genesis of listric faults, rather restricts solely to its shear heat estimation.

2. Model

We will derive an equation for shear heat produced by listric normal faults. The work considers slip along a stationary fault plane. We consider an arc of a circle, with radius/radius of curvature 'R', as a listric fault (Fig. 1a). Say by slipping the hanging wall block covered an angle

* Corresponding author.
E-mail addresses: soumyajitm@gmail.com, smukherjee@iitb.ac.in (S. Mukherjee).

https://doi.org/10.1016/j.marpetgeo.2018.09.004
Received 5 June 2018; Received in revised form 23 August 2018; Accepted 4 September 2018
Available online 05 September 2018

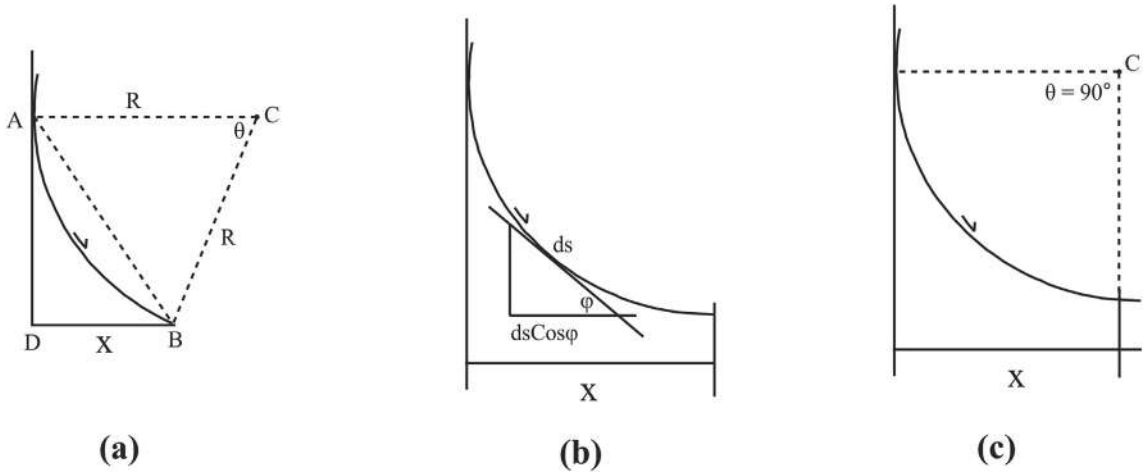

Fig. 1. a. For 'θ' amount of angular displacement of the hangingwall block, x' is the horizontal distance covered. 'C': center of circular arc-shaped listric fault plane. 'R': Radius (of curvature) of the fault plane. **Fig. 1b.** For a very small amount of slip 'ds' along the listric fault plane, the horizontal distance covered is 'dsCosΦ'. Φ: angle between the tangent at curved fault plane and a horizontal line. **Fig. 1c.** $\theta = l\,R^{-1}$ (l: arc length; R: radius). Putting l = 0.5 and 5 km in two trials, and θ = 90°; we get R = 0.318 and 3.18 km, respectively.

'θ' (in radian) over time 't'. Therefore, the length of arc covered over time 't' would be 'θR'. For a relative speed of slip 'v' between the hanging wall and the footwall block, this would mean:

$$\theta R = vt;\ \text{or}\ \theta = vt\,R^{-1} \quad (1)$$

Appendix explains the centripetal component of frictional force should be ignored in tectonic condition since it has a negligibly small magnitude.

Note faults can also follow a stick and slip mechanism whereby the magnitude of 'v' varies with time (Beeler et al., 2001), but we do not consider that in this work. The magnitude of work done ('dw') by such a movement, when 'F' is the frictional force:

$$dw = Fds \quad (2)$$

Here 'ds' stands for incremental displacement.

$$\text{And frictional force, } F = \mu mg Cos\Phi \quad (3)$$

Here *μ: coefficient of friction between the two blocks; m: mass of the hanging wall block; g: acceleration due to gravity;* Φ: angle between the tangent at point A and a horizontal line (Fig. 1b).

Putting the expression of F of eqn (3) into eqn (2):

$$dw = \mu mg Cos\Phi ds \quad (4)$$

$$\text{Therefore, total work done } W = \int dw = \mu mg \int Cos\Phi ds \quad (5)$$

$$\text{Now as per Fig. 1b, horizontal distance traveled by the hanging-wall block } x = \int Cos\Phi ds \quad (6)$$

$$\text{Therefore, } W = \mu mgx \quad (7)$$

As per geometry, inside triangle ABD: angle DAB = θ/2. Now, using sine rule inside triangle ABC:

$$AB/Sin\theta = BC/Cos\theta/2 \quad (8)$$

$$\text{Simplifying, } AB = 2RSin\theta/2 \quad (9)$$

$$\text{Inside triangle ADB: } Sin\theta/2 = BD/AB = x/(2RSin\theta/2);\ \text{or } x = 2RSin^2\theta/2 \quad (10)$$

Putting this expression of 'x' into eqn (7), and considering work done equals heat produced (Q):

$$Q = W = 2\mu mgRSin^2\theta/2 \quad (11)$$

However, this assumption would not work if fluids migrate along the fault, which would flush away the heat produced. Nevertheless, geo-modelers have produced W = Q models as a first approximation (e.g., Scholz, 1990). Such models would hold especially true for rocks with low thermal conductivities (λ) such as basalts ($\lambda = 1.7\,W\,m^{-1}\,K^{-1}$: Henderson and Henderson, 2009), or still better clay-dominated rocks ($\lambda = 0.6\,W\,m^{-1}\,K^{-1}$: Schon, 2011). On the other hand, rocks with high λ, e.g., quartzite (λ = 5.0: Henderson and Henderson, 2009) would deviate from the modeled shear heat.

Substituting the expression of 'θ' from eqn (1),

$$Q = 2\mu mgRSin^2vt/2R \quad (12)$$

3. Calculations

To present how shear heat increases with time, we consider the following parameters. The average frictional coefficient (μ) for rocks at geological deformation condition is ~0.3 (Byerlee, 1978). Listric faults in collisional tectonic regimes can remain active for several thousands of years or even more (Mukherjee, 2013a,b). Therefore, we will choose a time-scale for faulting for few thousands of years. We take the present day acceleration due to gravity $g = 980\,cm\,s^{-2}$, and an arbitrarily chosen 100 kg of point-mass ('m') of the hanging wall block. Slip rates ('v') for translational faults of various types have been deduced geo-chronologically, which usually range a few mm- (Dezes et al., 1999) up to a few cm per year (Kohn et al., 2004). We choose $v = 3\,mm\,yr^{-1}$ and $5\,cm\,yr^{-1}$ in different trials. Note that where the part of the listric fault has a low-dipping (~10°) fault plane, a slip rate as high as $\sim 2.5\,cm\,yr^{-1}$ might be acting (Buck, 1988). Healy et al. (2004) referred slip amounts of 0.5–5 km along listric faults at its different parts. Taking those magnitudes separately along a circular arc, and considering θ = 90° (or θ = π/2 radian) in Fig. 1c, we obtain R = 0.318 and 3.18 km, respectively. In four trials, with chosen parameters, the shear heat increases sigmoidally with time (Fig. 2a–d and their captions). In other words, shear heat initially increases rather slowly, and then it rises faster. Just as a single example, for the case of Fig. 2c (l = 0.5 km, R = 0.318 km, $v = 3\,mm\,yr^{-1}$, μ = 0.3, m = 100 kg), shear heat produced (H) is ~375 J. In this exercise, we are not able to choose all the parameters (right hand side of eqn (12)) from a single listric fault since all those parameters are not available from any single fault to our knowledge.

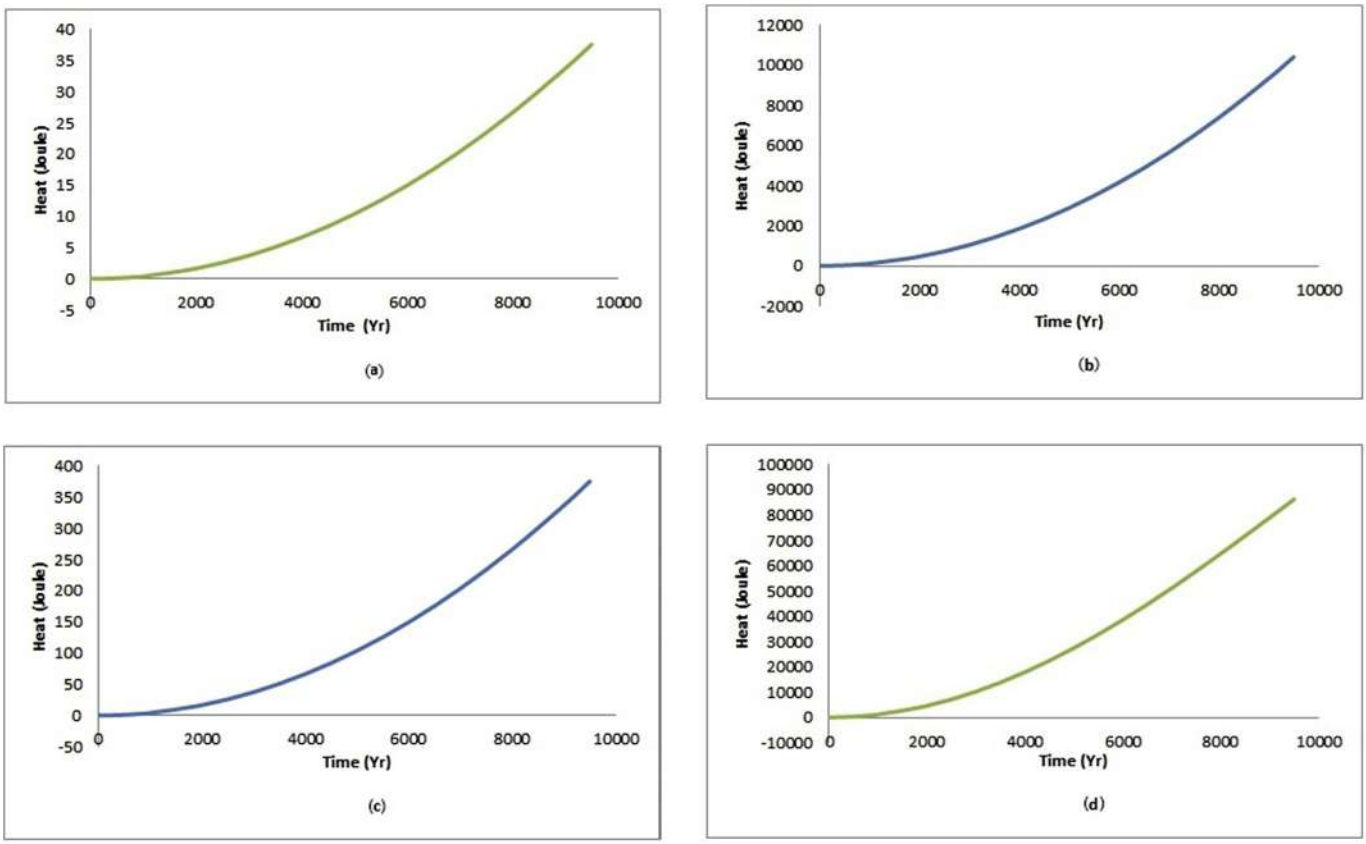

Fig. 2. Shear heat profiles with time, for m = 100 kg, μ = 0.3: **(a)** arc length (l) = 5 km for which R = 3.18 km, v = 3 mm yr^{-1}, **(b)** R = 3.18 km, v = 5 cm yr^{-1}, **(c)** arc length (l) = 0.5 km for which R = 0.318 km, v = 3 mm yr^{-1}, **(d)** arc length (l) = 0.5 km for which R = 0.318 km, v = 5 cm yr^{-1}.

4. Discussions and conclusions

We considered the curved fault plane to be a circular arc. Lohr et al. (2008) and Ellis and McClay (1988) also assumed cylindrical geometry of the fault plane while modeling listric fault kinematics. The hanging wall block is considered to slide downward relative to the footwall block with a constant velocity. This consideration is dissimilar to the case of free sliding of an object along a curved surface whereby the speed of slide changes due to variation in dip of the curved plane, as discussed in the dynamics texts (such as Das and Mukherjee, 2010). Also note that the issues of lithostatic- and tectonic pressures are taken care by considering the mass of the hanging wall block that slips over the fault plane, and the tectonic stress that causes faulting, respectively. As per eqn (12), shear heat is proportional to the coefficient of friction, mass of the hangingwall block and the radius (of curvature) of the circular fault plane. This is similar to the shear heat generated for rotational faults (eqns (10) and (11) of Khonsari and Mukherjee, submitted). $Q \propto \mu$ is as expected from common sense, and matches with the shear heat modeled for planar (dip slip) normal faults as done by Mukherjee (2017).

To better model shear heat (and kinematics) of listric faults, one can also find the best fit polynomial to represent the fault surfaces, as was done by Morris and Ferrill (1999) and Georgsen et al. (2012). Jones et al. (2000) presented how to find out the fault plane geometries, usually approximated as long wavelength and low amplitude curves, using terrestrial laser scanning technique. However, such an exercise may not give success, where the fault plane is exposed just as a line in a cross-section (Zhu et al., 2006). Listric faults with strike-slip (Vauchez and Brunel, 1988; Dorsey et al., 1995), oblique-slip (along with reverse slip) (Zhang et al., 2010), and even rotational slip (Wernicke and Burchfiel, 1982) have also been reported, and their shear heat budget needs to be determined separately. Listric faults that are produced merely by differential compaction of sediments across the fault planes along with some slip (such as the growth fault) would require a shear heat model different than what we propose here. One can deduce how shear heat produced by faulting would spread/dissipate in the fault rock, as the next step of study. Fundamentals of heat dissipation through rocks are already available (e.g., Lovering, 1935). For gouge-bearing faults, dissipation and production of shear heat would depend on fault zone structure and gouge-layer properties. Yang (2015) recently reviewed various fault zone structures. As per Rice (2006), the temperature of fault gouge is decided by shear heating and thermal diffusivity. In addition, hydraulic diffusivity would be an important parameter if fluid percolates through the damage zone adjoining the fault gouge. Since we do not have shear heat estimate of a listric fault at present, our calculated shear heat cannot be cross-checked immediately. Further, whether shear heat estimate will be dependent on normal or reverse drag (Mukherjee, 2014a,b) is not explored in the present "simple" model. A (listric) fault can disturb the local geothermal gradient due to movement of its faulted blocks. We do not bring this into our model as we intend to find out solely the shear heat related temperature rise and not the total temperature of the block.

A pseudotachylite-bearing fault zone connotes that the rock softened by partial melting that might have altered the thermal model in a more complicated manner than what is presented in this work. Therefore, strictly speaking, this work will hold true for those fault planes that are devoid of pseudotachylites.

Acknowledgements

IA worked as a Department of Science & Technology- Inspire Programme summer intern at IIT Bombay during May 2017. CPDA grant and the research sabbatical for the year 2017 received from IIT Bombay supported SM. Aayush Ranjan Keshav (IIT Kharagpur) is

thanked for interacting, especially regarding the derivations. Detail positive review by the two anonymous reviewers and the Handling Editor Adam Bumby are thanked.

Appendix

For a circular motion of a point mass that slides down, a "normal reaction" (N) works perpendicular to the plane (Appendix Fig. 1). Therefore,

$$N - mgCos\Phi = mv^2R^{-1} \quad (a1)$$

$$Or,\ N = mgCos\Phi + mv^2R^{-1} \quad (a2)$$

$$Now\ frictional\ force = \mu N = \mu mgCos\Phi + \mu mv^2R^{-1} \quad (a3)$$

Consideration of point mass in statics is customary. Taking the magnitude of parameters as Fig. 2d, the centripetal component of frictional force (μmv^2R^{-1}) comes out to be negligibly small ($2.4*10^{-19}$ N). If we choose magnitudes of μ, m and v (and R) smaller than (and greater than) Fig. 2d case, as in Fig. 2a–c, "μmv^2R^{-1}" further diminishes.

Appendix A. Supplementary data

Supplementary data related to this article can be found at https://doi.org/10.1016/j.marpetgeo.2018.09.004.

References

Beeler, N.M., Lockner, D.L., Hickman, S.H., 2001. A simple stick-slip and creep-slip model for repeating earthquakes and its implication for micro earthquakes at Parkfield. Bull. Seismol. Soc. Am. 91, 1797–1804.

Bertotti, G., terVoorde, M., 1994. Thermal effects of normal faulting during rifted basin formation, 2. The Lugano-Val Grande normal fault and the role of pre-existing thermal anomalies. Tectonophysics 240, 145–157.

Buck, W.R., 1988. Flexural rotation of normal faults. Tectonics 7, 959–973.

Byerlee, J.D., 1978. Friction of rocks Pure and Applied Geophysics. 116, 615–626.

Das, B.C., Mukherjee, B.N., 2010. In: Dynamics, twenty second ed. U.N. Dhur & Sons Private Ltd, pp. 314–315.

Dasgupta, S., Mukherjee, S., 2017. Brittle shear tectonics in a narrow continental rift: asymmetric non-volcanic Barmer basin (Rajasthan, India). J. Geol. 125, 561–591.

Dezes, P.J., Vannay, J.-C., Steck, A., Bussy, F., Cosca, M., 1999. Synorogenic extension: quantitative constraints on the age and displacement of the zanskar shear zone. Geol. Soc. Am. Bull. 111, 364–374.

Dorsey, R., Umhoefer, P.J., Renne, P.R., 1995. Rapid subsidence and stacked gilbert-type fan deltas, pliocene loreto basin, baja California sur, Mexico. Sediment. Geol. 98, 181–204.

Ellis, P.G., McClay, K.R., 1988. Listric extensional fault systems - results of analogue model experiments. Basin Res. 1, 55–70.

Fossen, H., 2016. In: Structural Geology, second ed. Cambridge University Press, Amsterdam, pp. 1–510.

Georgsen, F., Røe, P., Syversveen, A.R., Lia, O., 2012. Fault displacement modelling using 3D vector fields. Comput. Geosci. 16, 247–259.

Grasemann, B., Mancktelow, N.S., 1993. Two-dimensional thermal modelling of normal faulting: the simplon fault zone, central alps, Switzerland. Tectonophysics 225, 155–165.

Hamada, Y., et al., 2009. Estimated dynamic shear stress and frictional heat during the 1999 Taiwan Chi-Chi earthquake: a chemical kinetics approach with isothermal heating experiments. Tectonophysics 469, 73–84.

Harding, T.P., Lowell, J.D., 1979. Structural styles, their plate-tectonic habitats, and hydrocarbon traps in petroleum provinces. AAPG Bull. 63, 1016–1058.

Healy, D., Kusznir, N., Yielding, G., 2004. An inverse method to derive fault slip and geometry from seismically observed vertical stratigraphic displacements using elastic dislocation theory. Mar. Petrol. Geol. 21, 923–932.

Henderson, P., Henderson, G.M., 2009. In: The Cambridge Handbook of Earth Science Data. Cambridge University Press, pp. 73 ISBN 978-0-521-69317-2.

Hills, E.S., 2012. Elements of Structural Geology. Springer Science & Business Media.

Jones, R.R., Kokkalas, S., McKaffrey, K.J.M., 2000. Quantitative analysis and visualization of nonplanar fault surfaces using terrestrial laser scanning (LIDAR)—the Arkitsa fault, central Greece, as a case study. Geosphere 5, 465–482.

Kitamur, M., Mukoyoshi, H., Fulton, P.M., Hirose, T., 2012. Coal maturation by frictional heat during rapid fault slip. Geophys. Res. Lett. 39, L16302.

Kohn, M.J., Wieland, M.S., Parkinson, C.D., Upreti, B.N., 2004. Miocene faulting at plate tectonic velocity in the Himalaya of central Nepal. Earth Planet Sci. Lett. 228, 299–310.

Lohr, T., Krawczyk, C.M., Oncken, O., Tanner, D.C., 2008. Evolution of a fault surface from 3D attribute analysis and displacement measurements. J. Struct. Geol. 30, 690–700.

Lovering, T.S., 1935. Theory of heat conduction applied to geological problems. Geol. Soc. Am. Bull. 46, 69–94.

Mandal, S., Robinson, D., Khanal, S., Das, O., 2015. Redefining the tectonostratigraphic and structural architecture of the Almoraklippe and the Ramgarh–Munsiari thrust sheet in NW India. Geological Society, London, Special Publications 412, 247–269.

Morris, A.P., Ferrill, D.A., 1999. Constant-thickness deformation above curved normal faults. J. Struct. Geol. 21, 67–83.

Mukherjee, S., 2013a. Deformation Microstructures in Rocks 110 Springer ISBN 978-3-642-25608-0.

Mukherjee, S., 2013b. Channel flow extrusion model to constrain dynamic viscosity and Prandtl number of the Higher Himalayan Shear Zone. Int. J. Earth Sci. 102, 1811–1835.

Mukherjee, S., 2014a. Atlas of Shear Zone Structures in Meso-scales 73 Springer ISBN 978-3-319-0088-6.

Mukherjee, S., 2014b. Review of flanking structures in meso-and micro-scales. Geol. Mag. 151, 957–974.

Mukherjee, S., 2015. In: Atlas of Structural Geology. Elsevier, Amsterdam, pp. 88 ISBN: 978-0-12-420152-1.

Mukherjee, S., 2017. Shear heating by translational brittle reverse faulting along a single, sharp and straight fault plane. J. Earth Sys. Sci. 126 (1).

Mukherjee, S., Khonsari, M.M., 2017. Brittle rotational faults and the associated shear heating. Mar. Petrol. Geol. 88, 551–554.

Mukherjee, S., Khonsari, M.M., 2018. Inter-book normal fault-related shear heating in brittle bookshelf faults. Mar. Petrol. Geol. 97, 45–48.

Rice, J.R., 2006. Heating and weakening of faults during earthquake slip. J. Geophys. Res. 111 (B5).

Sakaguchi, A., Yanagihara, A., Ujiie, K., Tanaka, H., Kameyama, M., 2007. Thermal maturity of a fold–thrust belt based on vitrinite reflectance analysis in the Western Foothills complex, western Taiwan. Tectonophysics 443, 220–232.

Savage, H.M., Polissar, P.J., Sheppard, R., Rowe, C.D., Brodsky, E.E., 2014. Biomarkers heat up during earthquakes: new evidence of seismic slip in the rock record. Geology 42, 99–102.

Scholz, C.H., 1990. In: The Mechanics of Earthquakes and Faulting. Cambridge University Press, pp. 133–134.

Schon, J.H., 2011. Physical Properties of Rocks: a Workbook. Series Editor: Z J Cubitt. Handbook of Petroleum Exploration and Production 8. Elsevier, Amsterdam, pp. 347 ISBN: 978-0-444-53796-6.

Shelton, J.W., 1984. Listric normal faults: an illustrated summary. AAPG Bull. 68, 801–815.

Theunissen, K., Smirnova, L., Dehandschutter, B., 2002. Pseudotachylytes in the southern border fault of the Cenozoic intracontinental Teletsk basin (Altai, Russia). Tectonophysics 351, 169–180.

Underwood, M.B., Fulton, D.A., McDonald, K.W., 1988a. Thrust control on thermal maturity of the frontal Ouachita mountains, central Arkansas, USA. J. Petrol. Geol. 11, 325–340.

Underwood, M.B., O'Leary, J.D., Strong, R.H., 1988b. Contrasts in thermal maturity within terranes and across terrane boundaries of the Franciscan Complex, northern California. J. Geol. 96, 399–415.

Valdiya, K.S., Sanwal, J., 2017. In: Shroder Jr.J.F. (Ed.), Neotectonism in the Indian Subcontinent Landscape Evolution. Developments in Earth Surface Processes. 22. Elsevier, pp. 207–221.

Vauchez, A., Brunel, M., 1988. Polygenetic evolution and longitudinal transport within the Henderson mylonitic gneiss, North Carolina (southern Appalachian Piedmont). Geology 16, 1011–1014.

Wernicke, B., Burchfiel, B.C., 1982. Modes of extensional tectonics. J. Struct. Geol. 4, 105–115.

Wüstefeld, P., Hilse, U., Lüders, V., Wemmer, K., Koehrer, B., Hilgers, C., 2017. Kilometer-scale fault-related thermal anomalies in tight gas sandstones. Mar. Petrol. Geol. 86, 288–303.

Yamada, R., Ongirad, H., Matsuda, T., Omura, K., Takeuchi, A., Iwano, H., 2009. Fission track analysis of the Atotsugawa Fault (Hida Metamorphic Belt, central Japan: fault related thermal anomaly and activation history. In: Lisker, F., Ventura, B., Glasmacher, U.A. (Eds.), Thermochronological Method: from Palaeotemperature Constraints to Landscape Evolution Models. 324. Geol. Soc., Lond. Spec. Publ., pp. 331–337.

Yang, H., 2015. Recent advances in imaging crustal fault zones: a review. Earthq. Sci. https://doi.org/10.1007/s11589-015-0114-3.

Zhang, P.-Z., Wen, X., Shen, K., Chenm, J.-H., 2010. Oblique, high-angle, listric-reverse faulting and associated development of strain: the wenchuan earthquake of may 12, 2008, sichuan, China. Annu. Rev. Earth Planet Sci. 38, 353–382.

Zhu, L.-F., He, Z., Pan, X., Wu, X.-C., 2006. An approach to computer modeling of geological faults in 3D and an application. J. China Univ. Min. Technol. 16, 461–465.